AIAA 82-4116

Influence of Fabrication Tolerances on the Surface Accuracy of Large Antenna Structures

John M. Hedgepeth*
Astro Research Corporation, Carpinteria, Calif.

One of the sources of error in radio frequency antennas is the lack of dimensional precision of the surface. This paper presents an approach for estimating the amount of error caused by random dimensional imperfections of the many structural elements which make up a truss-type antenna. A principle of equivalence between the analyses of statistical errors and of the natural vibration frequencies of the structure is developed. Examples are presented to show the application of this equivalence principle to the determination of average surface errors of several types and proportions of antenna structures.

Introduction

STUDIES of the future missions for large space antennas have shown the need for very accurate antenna surfaces. In Ref. 1, for example, Freeland presents the accuracy requirements for a large variety of missions studied under the Large Space Systems Technology Program. He points out the need for antenna reflectors with diameter-to-surface-error ratios of 50,000, 100,000, or even 200,000. The approaches for achieving these desired accuracies are clearly of interest.

One approach to creating large accurate structures in space is to design the structure *and* the fabrication process so that individual parts can be made, with reasonable cost, accurately enough so that the assembly will meet its precision requirements. This straightforward procedure avoids expensive adjustment during and following assembly and has shown success in flight. An example is the extendible support structure shown in Fig. 1 which furnishes the backbone for the antenna panels on the Seasat synthetic aperture radar. This antenna is 10.75 m long and requires an accuracy of ± 6 mm from the support structure. By using graphite-composite material, a deep-truss configuration, and reasonably careful tooling, the accuracy requirement was easily met. Details of this structure are described in Ref. 2.

The Seasat task is much less demanding than that posed by the needs presented in Ref. 1. On the other hand, the effort required was also modest. How far can one go in meeting more difficult requirements?

A necessary ingredient in the answer to the question is the relationships between errors in the detailed parts and those in the assembled structure. If these relationships are known, then accurate estimates may be made of the surface accuracy yielded by a particular fabrication procedure. Alternatively, such information can be used to establish precision requirements on the fabrication procedures for desired missions.

The purpose of this paper is to examine these relationships for a particular type of structural configuration that is exemplified by the truss structure in Fig. 1 and the larger, more intricate lattice structures shown in Figs. 2 and 3. An analysis is made of the displacements caused by error strains in the individual members. Attention is directed to the situation in which the error strains result from fabrication tolerances and are therefore random variables. For a very general class of problems, the mean-square distortion of the surface is shown to be proportional to the sum of the inverse square of the vibration frequencies of the structure with an appropriately chosen mass distribution. This new result is applied to example cellular antenna structures, both flat and dished. Conclusions are drawn about the influence of overall dimension, local cell size, shell curvature and depth, and fabrication accuracy on the surface distortion.

Received May 6, 1980; revision received Sept. 22, 1981.

*President. Fellow AIAA.

Analysis

Define a three-dimensional lattice structure as an assemblage of straight members joined at node points in which the entire strain energy is equal to the sum of the extensional strain energies in the straight members. Note that this definition precludes bending or shearing strain energies in either the members or any reinforcing beams. Thus, for example, the definition implies that all joints carry no moment unless the adjacent members are rigid in bending. On the other hand, the definition clearly allows rigid boundaries, inserts, and reinforcing beams or rings, as well as force-free boundaries.

Although such a three-dimensional lattice structure can be very general in shape and composition, the purpose of the present study is to examine antenna support structures such as those in Figs. 1-3. The extendible support structure, the tetrahedral truss, and the geodesic dome are all three-dimensional lattice structures; they are also structures with a surface to which the antenna itself is attached. In the case of Fig. 1, the surface node points provide the mounting points for the phased-array antenna panels. In the case of Figs. 2 and 3, the surface nodes support a stretched reflector mesh.

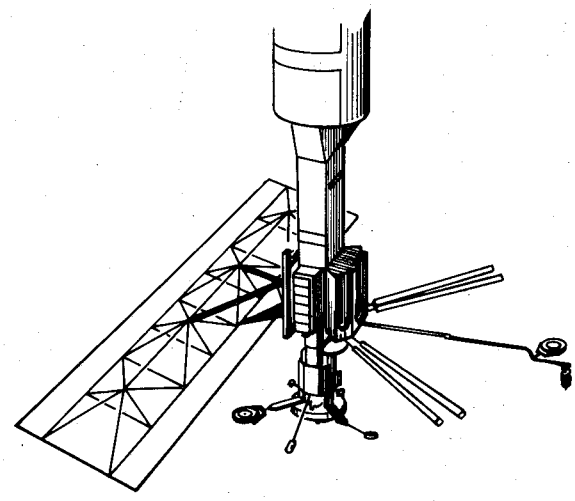

Fig. 1 Extendible support structure for Seasat synthetic aperture radar antenna.

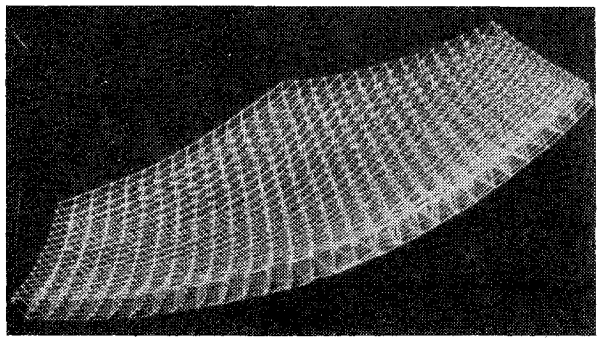

Fig. 2 Tetrahedral truss structure.

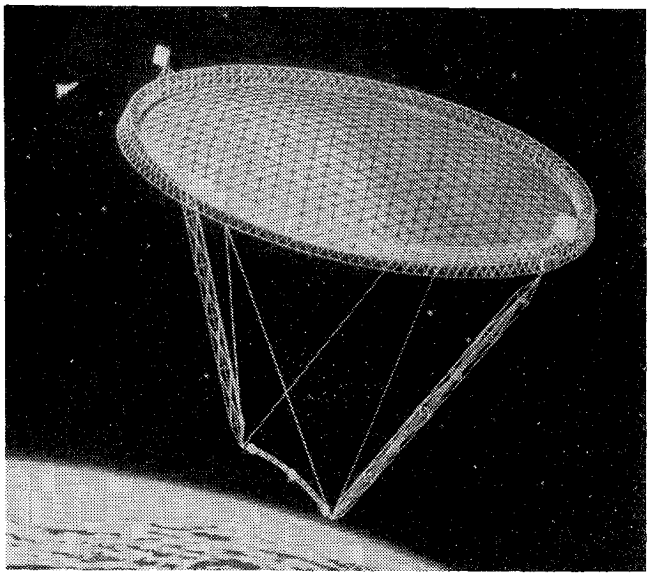

Fig. 3 Geodesic dome structure.

Dimensional errors in the structure affect the performance of the antenna by causing a distortion of the surface. The distortion primarily shifts the phase of the signal emitted locally from the surface by reflection or direct radiation. The detailed way in which the structural distortion changes the signal phase is dependent on the type of antenna. For a reflector, the important distortion is that normal to the surface; for a direct radiator, it is the axial distortion. Inasmuch as direct-radiating antennas are usually flat, the distortion perpendicular to the surface turns out to be the component of interest in both cases.

The degradation in antenna properties can be measured, in first approximation, in terms of the weighted average over the antenna aperture of the square of the phase deviation (see Ref. 3). This can be written in terms of the weighted mean square of the surface distortion $\overline{w^2}$ as

$$\overline{\delta^2} = (2\pi/\lambda)^2 C \overline{w^2} \tag{1}$$

where $\overline{\delta^2}$ is the weighted mean square of the phase deviation (in radian units), λ the wavelength, and C the multiplying factor which is approximately unity for a flat radiator and two for a reflector.

The weighted mean square of the surface deviation can be expressed in terms of the displacements of the lattice node points as follows.

Let u_m be the vector displacement of the mth node. Let A_m and $\hat{n}_m$ be the surface area and unit normal vector, respectively, for the surface nodes. Then

$$\overline{w^2} = \frac{1}{A} \sum_{m=1}^{M} f_m A_m (\hat{n}_m \cdot u_m)^2 \tag{2}$$

where A is the total surface area and f_m the weighting function which includes the effects of illumination distribution and nonperpendicular reflection. The function f_m is normalized so that

$$\frac{1}{A} \sum_{m=1}^{M} f_m A_m = 1 \tag{3}$$

In the analysis, attention is concentrated on situations in which the nodal displacements are caused by errors in the lengths of the lattice members. Let the number of such members be N and the unit error in the nth member ϵ_n. The load in the nth member can be expressed as

$$p_n = (EA)_n [E_n(|u|) - \epsilon_n] \tag{4}$$

where $E_n(|u|)$ is the strain in the nth member due to the displacements of its endpoints and $(EA)_n$ is the extensional stiffness of the nth member. The notation $|u|$ is used to signify the ordered set of all u_m, $m = 1,2...M$. The function E_n is assumed to be linear and homogeneous.

The equations of equilibrium at the nodes can be obtained from the variational principle

$$\delta(\text{S.E.}) = 0 \tag{5}$$

where S.E. is the gain in strain energy due to the displacements $|u|$. Thus,

$$\text{S.E.} = \frac{1}{2} \sum_{n=1}^{N} (EA)_n \ell_n \{[E_n(|u|)]^2 - 2\epsilon_n E_n(|u|)\} \tag{6}$$

where ℓ_n is the length of the nth member.

Of course, in performing the variation, the various constraints arising from rigid boundaries, stiffeners, and inserts must be observed. Constrained minimization of the strain energy with respect to the various displacement components would yield the desired equilibrium equations. The solution for the displacement components and substitution into Eq. (2) would then yield the desired result.

An alternative approach would be to use a modal solution. As will be seen, this approach has the advantage that published solutions of vibration problems can be used in solving the present problems. Furthermore, the modal approach allows the understanding of the surface-distortion problem to be assisted by analogy to an appropriate vibration problem.

Expand the displacement set in a series of orthogonal modes. Thus,

$$|u| = \sum_{i=1}^{I} a_i |U|_i \tag{7}$$

where the notation $|U|_i$ is again used to denote the ordered set of displacements U_{mi} at the mth node in the ith natural mode, and I is the total number of degrees of freedom of the nodes.

The several sets of orthogonal modes are obtained in the following way: For $i = 1,2,...,M$, the $|U|_i$ are solutions of the following expression of the Rayleigh-Ritz principle

$$\delta\left\{\frac{1}{2} \sum_{n=1}^{N} (EA)_n \ell_n [E_n(|U|)]^2 - \frac{1}{2}\omega^2 \sum_{m=1}^{M} f_m A_m (\hat{n}_m \cdot U_m)^2\right\} = 0 \tag{8}$$

The terms are seen to be the maximum potential and kinetic energies during sinusoidal vibration. Note that the weighting function f_m takes on the role of the mass per unit area. Note also that inertia forces tangent to the surface are ignored.

The eigensolutions of Eq. (8) are scaled to form an orthonormal set. Thus,

$$\frac{1}{A}\sum_{m=1}^{M} f_m A_m (\hat{n}_m \cdot U_{m_i})(\hat{n}_m \cdot U_{m_j}) = 1, \quad i=j$$
$$= 0, \quad i \neq j \tag{9}$$

The eigenfunctions also diagonalize the potential energy. That is,

$$\frac{1}{A}\sum_{n=1}^{N} (EA)_n \ell_n E_n(|U|_i) E_n(|U|_j) = \omega_i^2, \quad i=j$$
$$= 0, \quad i \neq j \tag{10}$$

The number of members of the set of eigenfunctions is equal to the number M of surface nodes which, in general, is less than the number of degrees of freedom. The set is complete to the extent of expressing the normal surface displacement, but it is not able, in general, to express the vector displacements of all the nodes. In order to make the total set used in Eq. (7) complete, $(I-M)$ additional functions must be generated. These additional functions must have null normal displacement of the surface nodes, inasmuch as the M eigenfunctions constitute a complete set with respect to these displacements. In addition, they can be constructed so that they are orthogonal to the vibration eigenfunctions and to each other with respect to the potential energy. Note that these additional orthogonal modes have infinite natural frequencies and therefore do not enter into the following results; their evaluation is accordingly unnecessary.

Substituting the expansion [Eq. (7)] into the expression for $\overline{w^2}$ [Eq. (2)] and using Eq. (9) gives

$$\overline{w^2} = \sum_{i=1}^{M} a_i^2 \tag{11}$$

Similarly, substituting Eq. (7) into the strain energy [Eq. (6)] and applying Eq. (10) gives

$$\text{S.E.} = \frac{1}{2}\sum_{i=1}^{M} A\omega_i^2 a_i^2 + \frac{1}{2}\sum_{i=M+1}^{I} a_i^2 \sum_{n=1}^{N} (EA)_n \ell_n [E_n(|U|_i)]^2$$
$$- \sum_{i=1}^{I} a_i \sum_{n=1}^{N} (EA)_n \ell_n \epsilon_n E_n(|U|_i) \tag{12}$$

where the linear homogeneous property of E_n has been used. Minimizing with respect to a_i $(i=1, M)$ gives

$$a_i = \frac{1}{A\omega_i^2}\sum_{n=1}^{N} (EA)_n \ell_n \epsilon_n E_n(|U|_i) \tag{13}$$

The expression $(EA)_n E_n(|U|_i)$ can be recognized as the load distribution P_{n_i} in the members for the deflection shape of the ith mode. Thus,

$$a_i = \frac{1}{A\omega_i^2}\sum_{n=1}^{N} P_{n_i} \ell_n \epsilon_n \tag{14}$$

For a known pattern of built-in strains ϵ_n, the coefficients can be evaluated by Eq. (13) or (14) and substituted into Eq. (11) to obtain the desired result.

In this paper attention is directed to the case where the ϵ_n arise from random fabrication errors and, therefore, are independent random variables. Let them each have a zero mean and a standard deviation of σ_{ϵ_n}. Then the expected value or "expectation" of $\overline{w^2}$ is

$$\langle \overline{w^2} \rangle = \sum_{i=1}^{M} \langle a_i^2 \rangle \tag{15}$$

where

$$\langle a_i^2 \rangle = \frac{1}{A^2\omega_i^4}\sum_{n=1}^{N} (EA)_n^2 \ell_n^2 \sigma_{\epsilon_n}^2 [E_n|U|_i]^2 \tag{16}$$

in which the statistical independence of ϵ_n and ϵ_m has been used to collapse the double summation into the single one. The expression for $\langle \overline{w^2} \rangle$ can also be written

$$\langle \overline{w^2} \rangle = \frac{1}{A^2}\sum_{n=1}^{N} \ell_n^2 \sigma_{\epsilon_n}^2 \sum_{i=1}^{M} \frac{P_{n_i}^2}{\omega_i^4} \tag{17}$$

The expectation of $\overline{w^2}$ can be calculated for known distribution of σ_{ϵ_n} from this expression. If the distribution of σ_{ϵ_n} has a particular form, the result is extremely simple. In order to obtain this, let $\overline{EA}$, ℓ, and σ_ϵ be reference values. Then set

$$\sigma_{\epsilon_n}^2 = \frac{\overline{EA}\,\ell}{(EA)_n \ell_n}\sigma_\epsilon^2 \tag{18}$$

Applying Eq. (10) yields

$$\langle a_i^2 \rangle = \frac{\overline{EA}\,\ell\sigma_\epsilon^2}{A\omega_i^2} \tag{19}$$

Substituting into Eq. (15) yields finally

$$\langle \overline{w^2} \rangle = \frac{\overline{EA}\,\ell\sigma_\epsilon^2}{A}\sum_{i=1}^{M} \frac{1}{\omega_i^2} \tag{20}$$

Thus, the mean square surface distortion is expressed as the sum of the inverse squares of the natural frequencies of the structure with appropriately chosen masses. The usefulness of this remarkable result is illustrated in the next section.

Applications

Consider a three-dimensional lattice structure in the form of a shell in which the surfaces are triangular lattices of the open "isogrid" type. Assume that the shell is composed of a large number of cells and is thin enough that its deformations can be expressed in terms of a displacement and rotation of an equivalent cross section. Then the vibration characteristics of this "lattice" shell can be estimated by examining the vibration characteristics of an equivalent continuous isotropic shell that has the following properties (see Ref. 3)

Shell bending stiffness:

$$D_s = \frac{3\sqrt{3}}{8}\frac{EAH^2}{\ell} \tag{21}$$

Shell membrane stiffness:

$$(Eh)_s = \frac{4}{\sqrt{3}}\frac{EA}{\ell} \tag{22}$$

Shell shear stiffness:

$$(Gh)_s = \frac{EAH^2}{\sqrt{3}(H^2+\ell^2/3)^{3/2}} \tag{23}$$

Shell Poisson's ratio:

$$\nu_s = 1/3 \tag{24}$$

Shell unit mass:

$$\rho_s = f \tag{25}$$

In these formulas, EA and ℓ are lattice properties as before, H the shell depth, and f the weighting function. In general, these quantities may all vary over the lattice surface; the shell stiffness and unit mass D_s and m_s would vary accordingly. In many cases, the variation of lattice properties is not large. Furthermore, useful results can be obtained for a uniform weighting function. Therefore, the vibration solutions for uniform shells can be used to advantage.

The process to be followed is straightforward. First, identify an equivalent shell vibration problem. Then determine the natural frequencies. Finally, sum their squared reciprocals and substitute into Eq. (20) to estimate the surface distortion.

Some care must be exercised in selecting the appropriate boundary conditions. In most cases, for example, the "rigid-body" components of displacement are not important and free-free conditions should be used. On the other hand, if displacements with respect to particular points are of interest, then the shell should be assumed to be supported at those points. The influence of a rigid rim can be incorporated by requiring that the boundary move as a massless rigid body.

Another complication arises from the fact that the truss structure has a finite number of vibration modes, whereas the equivalent "smeared out" structure has an infinite number. The validity of the equivalence is thus questionable for the higher modes. For situations for which the vibration frequencies increase rapidly, the resulting errors are unimportant; indeed, a useful approximation can be obtained by summing [in Eq. (20)] over an infinite number of modes. On the other hand, for situations where the increase is slow, the summation should include only the correct finite number of modes. Some error is clearly introduced by the inaccuracy of the equivalence. Furthermore, some arbitrary decisions must be made as to *which* modes are to be included. Nevertheless, results can be obtained which should be useful at least for conceptual design. Some example applications follow.

Circular Tetrahedral Truss

Consider a tetrahedral truss with a circular planform. Assume the truss to be flat, or with small enough curvature so that it can be treated as being flat. The equivalent "smeared out" structure is a circular plate with free-free boundary conditions. If the truss is thin enough, then the effects of transverse shear in the equivalent plate are ignorable. The frequencies are therefore those of a free-free circular plate as treated in Ref. 4. In that paper, the frequencies are expressed in terms of the tabulated parameter λ as follows:

$$\omega^2 = (D_s/\rho_s a^4)\lambda^4 \tag{26}$$

where a is the radius. Substituting in Eq. (20) and using Eqs. (21) and (25) (with $f=1$) gives

$$\frac{\langle \overline{w^2} \rangle}{D^2} = \frac{2\sqrt{3}}{9\pi}\frac{\ell^2}{H^2}\sigma_\epsilon^2 \sum_{i=1}^{M} \frac{1}{\lambda_i^4} \tag{27}$$

where D is the diameter of the reflector.

The values of λ_i for a free-free circular plate are tabulated in Table 2.9 of Ref. 4. In performing the summation in Eq. (27), the terms for $n=0$ are included once but the terms for $n\neq 0$ are counted twice, once each for the modes corresponding to $\cos n\theta$ and $\sin n\theta$. Following that procedure and summing over all the tabulated entries gives

$$\sum \frac{1}{\lambda_i^4} = 0.116$$

of which the biggest contribution (0.075) comes from the $n=2$ modes. Practical convergence is demonstrated by the fact that the $n=6$ modes contribute only 0.001. Incidentally, the dominance of the $n=2$ modes in the summation implies that the shape of the surface error is primarily composed of $n=2$ modes.

Substituting the value of the summation gives

$$\sqrt{\langle \overline{w^2} \rangle}/D = 0.119(\ell/H)\sigma_\epsilon \tag{28}$$

for the circular tetrahedral truss with a free unreinforced rim.

Now, consider a circular tetrahedral truss with a rim held to be error free. The analogous continuous vibration problem is that of a plate with a rigid ring at the rim. If the combined plate-ring is free, then the frequencies are appropriate to the case where rigid-body components of the surface error are not important. For $n=0$ and 1 the frequencies are, of course, the same as those for the free unreinforced plate. For $n\geq 2$, the frequencies are those of a simply supported circular plate which can be obtained from Table 2.3 of Ref. 4 as augmented by appropriate asymptotic approximations to achieve convergence. Carrying out the summation yields

$$\sqrt{\langle \overline{w^2} \rangle}/D = 0.056(\ell/H)\sigma_\epsilon \tag{29}$$

for the circular tetrahedral truss with a free zero-error edge.

If the rigid-body components of error are of concern, then their effect can be obtained by using the simply supported frequencies as appropriate. For example, if the tilt components are included and the rim is error free, the frequency values for $n=1$ should be those for the simply supported plate. The result is

$$\sqrt{\langle \overline{w^2} \rangle}/D = 0.062(\ell/H)\sigma_\epsilon \tag{30}$$

for the circular tetrahedral truss with a zero-error edge and tilt components included.

If all the rigid-body components are important, then the simply supported frequencies should be used for all modes. This yields

$$\sqrt{\langle \overline{w^2} \rangle}/D = 0.084(\ell/H)\sigma_\epsilon \tag{31}$$

for the circular tetrahedral truss with a zero-error edge and all rigid-body components included.

Deep Tetrahedral Truss

For a deep truss, the effects of errors in the intersurface members become important. The equivalent vibration problem is that of a plate with transverse shear. Unfortunately, in the literature the effects of transverse shear are usually considered in conjunction with the equally important effects of rotary inertia. So the simpler problem is not treated.

In order to get an approximate measure of the effects of transverse shear alone, consider the vibration of a square plate with simple-support boundary conditions. The differential equations for this problem are given in Sec. 12.3 of Ref. 4 with the rotary-inertia terms set equal to zero. With the notation of that reference and for the domain shown in Fig. 4,

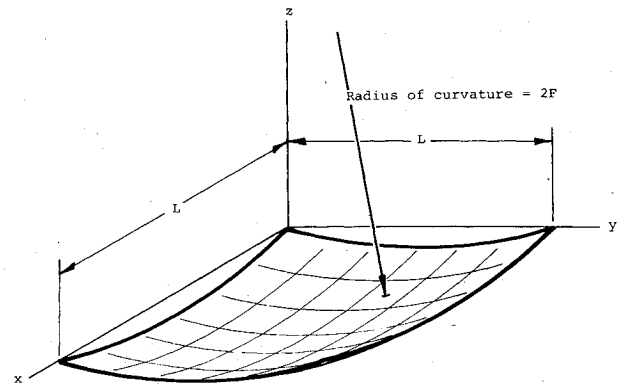

Fig. 4 Square-aperture notation.

let

$$w = W_0 \sin(m\pi x/L)\sin(n\pi y/L)$$

$$H = H_0 \sin(m\pi x/L)\sin(n\pi y/L) \tag{32}$$

which are exact solutions for simply supported edges. Then the square of the vibration frequency is

$$\omega^2 = \frac{D_s\pi^4}{\rho_s L^4}\left\{(m^2+n^2)^2 \Big/ \left[1+\frac{D_s\pi^2}{(Gh)_s L^2}(m^2+n^2)\right]\right\} \tag{33}$$

where the notation is now that of the present paper.

Substituting into Eq. (20) and using Eqs. (21), (23), and (25) (with $f=1$) yields

$$\frac{\langle \overline{w^2}\rangle}{D_{\text{eff}}^2} = \frac{2\sqrt{3}}{9\pi^3}\left(\frac{\ell}{H}\right)^2 \sigma_\epsilon^2 \sum_{m=1}^{\sqrt{M}}\sum_{n=1}^{\sqrt{M}} \frac{1}{(m^2+n^2)^2} + \frac{\sqrt{3}}{\pi^2}\frac{H}{\ell}$$

$$\times\left(1+\frac{1}{3}\frac{\ell^2}{H^2}\right)^{3/2}\sigma_\epsilon^2\left(\frac{\ell}{D_{\text{eff}}}\right)^2 \sum_{m=1}^{\sqrt{M}}\sum_{n=1}^{\sqrt{M}} \frac{1}{m^2+n^2} \tag{34}$$

where D_{eff} is the diameter of the circular aperture of the same area as the square and, as before, M is the number of surface nodes. [See the discussion following Eq. (35).] The summations are carried out over a total of M terms. Note that the first term gives the contribution of random errors in the surface members and the second term shows the effect of errors in the intersurface members.

For large M, the summation in the first term converges rapidly. In fact, for $M=25$, the summation is 0.4053, which is only 4% less than the converged value of 0.4244. On the other hand, the summation in the second term diverges as $M\to\infty$. The influence of the errors in the intersurface members therefore depends on the number of the surface nodes, which is the ratio of approximately the surface area $\pi D^2/4$ divided by the nodal area $\sqrt{3}\ell^2/2$.

$$M \approx (\sqrt{3}\pi)/6(\ell/D_{\text{eff}})^2 \tag{35}$$

Recall that the approach is valid only for large M. The error is small therefore if M is chosen to be the perfect square nearest to the right-hand side of Eq. (35).

For M large, the mean-square error can be written in the form

$$\frac{\langle \overline{w^2}\rangle}{D_{\text{eff}}^2} = \left(0.073\frac{\ell}{H}\sigma_\epsilon\right)^2 + \frac{\langle \overline{w^2}\rangle_I}{D_{\text{eff}}^2} \tag{36}$$

where the contribution of the errors in the intersurface members is

$$\frac{\langle \overline{w^2}\rangle_I}{D_{\text{eff}}^2} = \left[G_1\left(\frac{\ell}{H}\right)G_2\left(\frac{\ell}{D_{\text{eff}}}\right)\frac{\ell}{H}\sigma_\epsilon\right]^2 \tag{37}$$

In this expression

$$G_1\left(\frac{\ell}{H}\right) = \left(\frac{3}{4}\frac{H^2}{\ell^2}+\frac{1}{4}\right)^{3/4} \tag{38}$$

$$G_2\left(\frac{\ell}{D_{\text{eff}}}\right) = \sqrt{\frac{8}{3\pi^2}\left(\frac{\ell}{D_{\text{eff}}}\right)^2 \sum_{m=1}^{\sqrt{M}}\sum_{n=1}^{\sqrt{M}} \frac{1}{m^2+n^2}} \tag{39}$$

The functions G_1 and G_2 are plotted in Fig. 5.

The first term in the mean-squared error can be compared with the similar result for the circular plate, Eq. (31). The two results are close to each other. Useful approximations can evidently be made by analyzing equivalent-area aperture shapes.

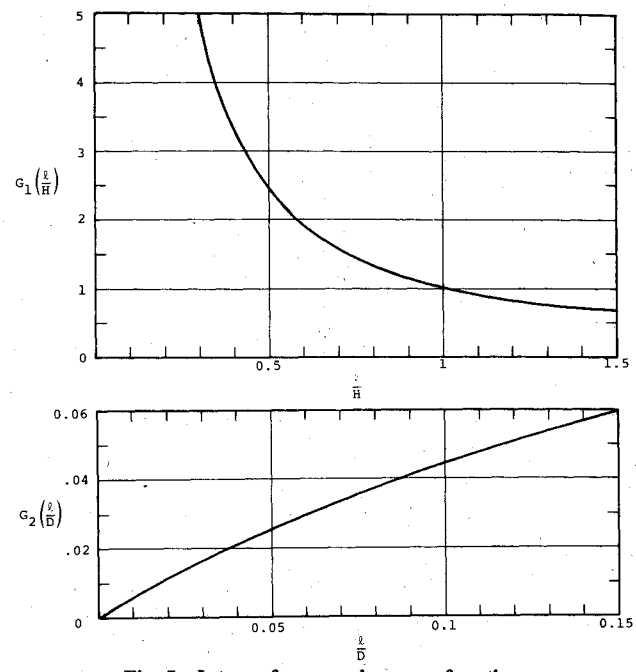

Fig. 5 Intersurface-member error functions.

The added effect of intersurface-member error is exhibited in Eq. (37) in such a manner as to permit easy comparison with the other results. The coefficient function G_1 has a value of unity for $\ell/H=1$; thus, the function G_2 can be compared directly with the coefficients in Eqs. (28-31) for $\ell/H=1$.

Several observations are appropriate here. First, in the absence of better data, the predictions of Eq. (37) can be used to estimate the influence of intersurface-member error for a wide variety of planforms and boundary conditions inasmuch as these effects tend to be localized. Second, the contribution is smaller than that of the surface-member error for $\ell/H=1$ even for $\ell/D<0.03$. Third, increasing the depth of the truss should be done with caution since the contribution increases very rapidly.

Truss Dishes

Reflector antennas need to be shaped as paraboloids or near-paraboloids with radii of curvature approximately equal to twice the focal length F. For a truss-type reflector without reinforcement at the rim, the vibration (and hence error) behavior should be approximated well by the flat-truss results obtained previously unless the F/D ratio is small. If the rim is held error free, on the other hand, the effects of shell curvature can be profound.

Clearly, the equivalent continuous structure to analyze is the spherical shell with simply supported edges and with properties as given in Eqs. (21-25). The vibrations of such a shell with a square planform have been treated by Reissner in Ref. 5. His results can be used directly here because he includes only the effects of lateral inertia which the present analysis centers upon. In the notation of this paper, the result of Ref. 5 is

$$\omega_{mn}^2 = \frac{3\sqrt{3}\pi^4}{8}\frac{EAH^2}{\ell L^4}(m^2+n^2) + \frac{\sqrt{3}}{3}\frac{EA}{\ell F^2} \tag{40}$$

where m and n are the mode numbers as in Eq. (33) and L is again the size of the square aperture. Note that the first term arises from the bending stiffness of the shell and the second contains the effects of curvature.

Substituting into Eq. (20) gives

$$\frac{\langle w^2\rangle}{D_{\text{eff}}^2} = \frac{2\sqrt{3}}{9\pi^3}\left(\frac{\ell}{H}\right)^2 \sigma_\epsilon^2 \sum_{m=1}^{\sqrt{M}}\sum_{n=1}^{\sqrt{M}} \frac{1}{(m^2+n^2)^2+Z^2} \tag{41}$$

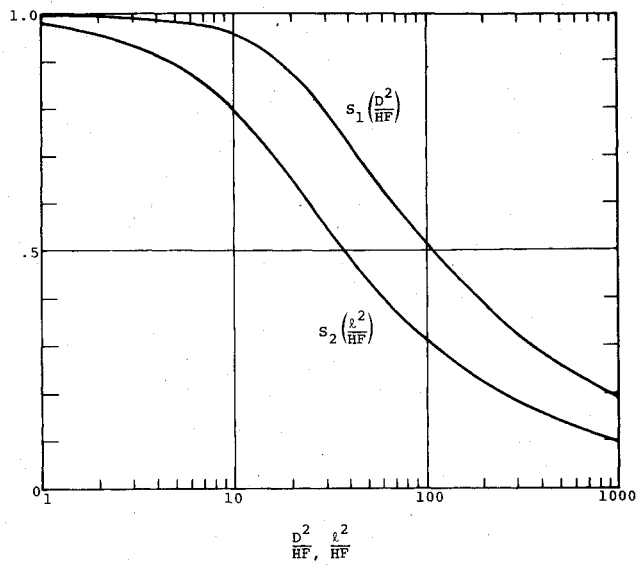

Fig. 6 Truss-shell curvature functions.

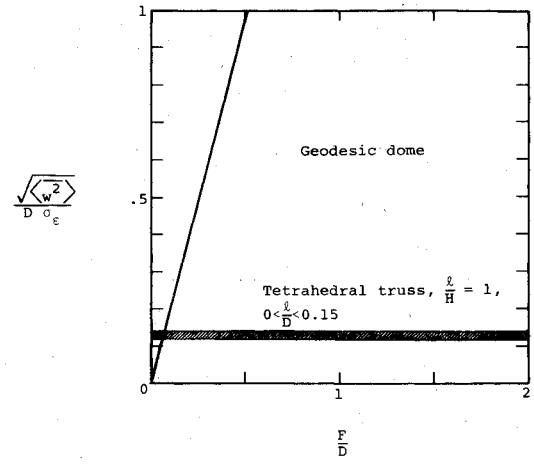

Fig. 7 Surface errors for two configurations.

where the curvature parameter Z is

$$Z=\frac{\sqrt{2}}{6\pi}\frac{D_{\text{eff}}^2}{HF} \tag{42}$$

D_{eff} is the diameter of the equal-area circle and M is again the number of surface nodes [see Eq. (35)].

For ease of comparison with the previous results, let

$$S_M(Z)=\left[\frac{2\sqrt{3}}{9\pi^3}\sum_{m=1}^{\sqrt{M}}\sum_{n=1}^{\sqrt{M}}\frac{1}{(m^2+n^2)^2+Z^2}\right]^{1/2} \tag{43}$$

Then

$$\frac{\langle \overline{w^2} \rangle}{D_{\text{eff}}}=\left[S_M(Z)\frac{\ell}{H}\sigma_\epsilon\right]^2 \tag{44}$$

for the spherical truss shell with a zero-error rim.

Calculations show that the coefficient $S_M(Z)$ is approximated well by

$$S_M(Z)=0.073S_1\left(\frac{D_{\text{eff}}^2}{HF}\right)S_2\left(\frac{\ell^2}{HF}\right) \tag{45}$$

where S_1 and S_2 are plotted in Fig. 6. In the limit of large F, the functions S_1 and S_2 both approach unity. The surface error therefore approaches that of the flat truss, as it should [see Eq. (36)].

Another interesting limit is obtained when the truss H is allowed to approach zero. Then the truss shell becomes a geodesic dome which depends on the combination of shell curvature and membrane stiffness for its structural integrity. Examination of Eq. (40) shows that the vibration frequencies of a membrane structure are independent of the mode wavelength. The evaluation of the surface error is then a simple matter of multiplying the reciprocal frequency squared by the number of surface nodes. Because a geodesic dome has only one surface lattice, the membrane stiffness in Eq. (22), and hence Eq. (40), must be cut in half. The process yields

$$\frac{\sqrt{\langle \overline{w^2} \rangle}}{D_{\text{eff}}}=\frac{2F}{D_{\text{eff}}}\sigma_\epsilon \tag{46}$$

for the geodesic dome with a zero-error rim.

This remarkably simple result allows the estimation of the potential surface accuracy of single-layer truss structures

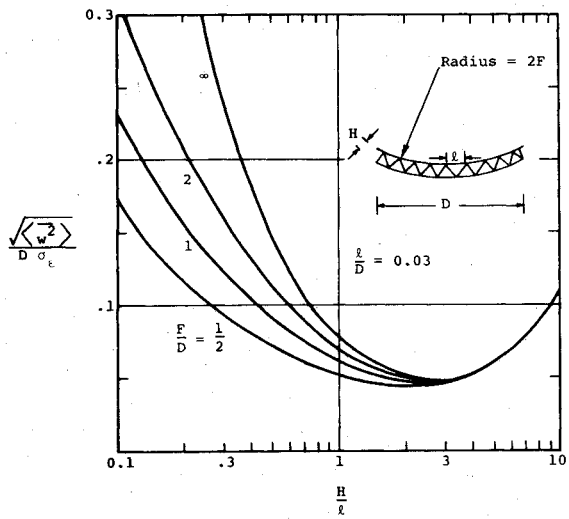

Fig. 8 Effect of truss-shell depth and curvature on surface errors.

which are of interest because they have fewer members than the full truss. It is very nearly the same as the estimate obtained in the previous treatment of Ref. 6. In that paper, a shallow spherical isogrid lattice with an infinite domain is analyzed. Comparison of the present results with those of that paper shows that the effect of the rigid rim is to cut the rms error by only about 10%.

Concluding Discussion

The approach described in this paper is particularly useful in the early stages of design in which not only the structural proportions are being sought, but also the type of structure is undecided. As an example of the latter application, Fig. 7 has been prepared to compare the surface errors of the two structural types of Figs. 2 and 3. For small values of F/D, the two types yield similar accuracy, whereas the geodesic dome exhibits increasing error as F/D increases. If high accuracy is required, therefore, the tetrahedral truss would be the better choice even though it is more complex, unless the reflector dish were very deep. On the other hand, if error/diameter ratios equal to the possible unit fabrication errors are acceptable, then either concept could be used for $F/D<1$.

The proportion selection process is also aided. For example, the combined effects of truss depth and shell curvature are shown in Fig. 8 for the tetrahedral truss structure

with a stabilized rim. The results include the influence of intersurface-member errors by adding the mean-square error of Eq. (37) to that of Eq. (44). A value of ℓ/D of 0.03 is arbitrarily selected for all the curves. The rms error is shown as a function of the ratio of depth to element length for several shell curvatures (expressed in terms of the F/D ratio).

As expected, the effects of curvature are especially important for the thin shells. The surface error is a minimum at around $H/\ell=3$. For these deeper trusses, the effects of curvature are small, even for $F/D=1/2$.

Acknowledgment

This work was performed under Contract NAS1-15347 from NASA Langley Research Center.

References

[1] Freeland, R. E., "Industry Capability for Large Space Antenna Structures," Jet Propulsion Laboratory, Rept. 710-12, May 25, 1978.

[2] Campbell, B. E. and Hawkins, W., "An 11-Meter Deployable Truss for the Seasat Radar Antenna," Paper presented at the 12th Aerospace Mechanisms Symposium, NASA Ames, April 1978.

[3] Mikulas, M. M. Jr., Bush, H. G., and Card, M. F., "Structural Stiffness, Strength and Dynamic Characteristics of Large Tetrahedral Space Truss Structures," NASA TM-X-74001, 1977.

[4] Leissa, A. W., "Vibration of Plates," NASA SP-160, 1969.

[5] Reissner, E., "On Transverse Vibrations of Thin, Shallow Elastic Shells," *Quarterly Journal of Applied Mathematics*, Vol. 13, No. 2, July 1955, pp. 169-176.

[6] Hedgepeth, J. M. and Miller, R. R., "Effect of Member-Length Imperfections on the Deformations and Loads in an Isogrid-Truss Structure," Astro Research Corp., ARC-R-1012, April 1, 1980.